Effective Concentrations of Amino Acid Side Chains in an Unfolded Protein†

Kamalam Muthukrishnan‡ and Barry T. Nall*
Department of Biochemistry, University of Texas Health Science Center, San Antonio, Texas 78284
Received December 18, 1990; Revised Manuscript Received February 21, 1991

ABSTRACT: Preferential interactions between chain segments are studied in unfolded cytochrome *c*. The method takes advantage of heme ligation in the unfolded protein, a feature unique to proteins with covalently attached heme. The approach allows estimation of the effective concentration of one polypeptide chain segment relative to another, and is successful in detecting differences for peptide chain segments separated by different numbers of residues in the linear sequence. The method uses proton NMR spectroscopy to monitor displacement of the histidine heme ligands by imidazole as guanidine hydrochloride unfolded cytochrome *c* is titrated with deuterated imidazole. When the imidazole concentration exceeds the effective (local) concentration of histidine ligands, the protein ligands are displaced by deuterated imidazole. On displacement, the histidine ring proton resonances move from the paramagnetic region of the spectrum to the diamagnetic region. Titrations have been carried out for members of the mitochondrial cytochrome *c* family that contain different numbers of histidine residues. These include cytochromes *c* from tuna (2), yeast iso-2 (3), and yeast iso-1-MS (4). At high imidazole concentration, the number of proton resonances that appear in the histidine ring C_2H region of the NMR spectrum is one less than the number of histidine residues in the protein. So one histidine, probably His-18, remains as a heme ligand. The effective local concentrations of histidines-26, -33, and -39 relative to the heme (position 14–17) are estimated to be (3–16) $\times 10^{-3}$ M. Tentative residue-specific resonance assignments for the displaced histidine C_2H ring protons suggest that the effective concentrations of histidine side chains relative to the heme have the order: His-18 $\gg$ His-26 $>$ His-33 $\sim$ His-39. For cytochromes *c* with more than two histidine side chains, there are more heme ligands than heme coordination sites. While ligation preferences are discernible, there is sharing of coordination sites among the available histidine ligands. While it is clear that imidazole titrations are capable of detecting structure in unfolded cytochrome *c*, present results at high denaturant concentrations are largely consistent with those expected for a random-coil polypeptide chain.

Retention of a functional tertiary structure in a globular protein requires a favorable balance between factors that influence the relative stabilities of competing active and inactive conformations. In attempts to reconcile structural and stability differences in mutant proteins, most attention has been directed toward mutation-induced differences in the folded forms, usually as determined by X-ray crystallography. The other half of the problem, characterization of mutation-induced differences in unfolded proteins, has received relatively little attention for at least two reasons. First, the properties of unfolded proteins are often assumed to resemble those of a random-coil polymer, and for random-coil polymers, mutation-induced stability differences are likely to be small. Second, there are considerable experimental difficulties in characterizing unfolded proteins by methods that do not presuppose statistical behavior of the polymer segments. As a result, there have been few critical tests for deviations from the random-coil model.

For small water-soluble globular proteins, the simplest possible model, a two-state model, provides an excellent approximation to the complex molecular conformational changes that occur during protein folding (Brandts, 1969). The two-state model of folding postulates two thermodynamically important states at equilibrium: the functional folded state and the inactive unfolded state. An understanding of protein stability is reduced to the problem of measuring the factors influencing the relative stabilities of the folded and unfolded states of a protein. Recent experimental work on stabilities of mutant proteins has validated further the two-state model, but the randomness of unfolded states has come under suspicion. There is increasing evidence that the heterogeneous character of protein sequences leads to strongly preferred interactions in unfolded polypeptides, even under highly denaturing conditions. Moreover, striking differences in the susceptibility of mutant proteins to strong denaturants have been attributed to mutation-induced changes in interactions of hydrophobic side chains in the unfolded state (Shortle & Meeker, 1986, 1989). Thus, characterization of the unfolded states of proteins has gained in importance.

Cytochrome *c* is unusual in that it contains a heme as a covalently attached prosthetic group. Heme ligation by nitrogen-containing or sulfur-containing protein side chains is important to the folded form of cytochrome *c* and also the unfolded state (Babul & Stellwagen, 1971). Even the protein folding process, as judged from folding rates and amplitudes, is altered in the presence of small molecules or ions capable of heme ligation (Brems & Stellwagen, 1983; Myer, 1984). Heme ligation adds to the complexity of unfolded cytochrome *c*, but ligation also provides a means of estimating effective concentrations of unfolded polypeptide chain segments. The method, titration of cytochrome *c* with a small-molecule heme ligand, is simple and has often been used to study heme ligation in folded heme-containing proteins. In the present case, the chemistry of ligation by the extrinsic ligand, imidazole, is similar to that of ligation by the intrinsic histidine side chains in unfolded cytochrome *c*. Thus, the imidazole concentration needed to displace a histidine ligand should be a measure of

† Supported by grants from the National Institute of General Medical Sciences (GM 32980) and the Robert A. Welch Foundation (AQ 838).
* Address correspondence to this author at the Department of Biochemistry, University of Texas Health Science Center, 7703 Floyd Curl Dr., San Antonio, TX 78284-7760.
‡ Present address: Department of Biochemistry, Rice University, Houston, TX 77251.

0006-2960/91/0430-4706$02.50/0

the (intramolecular) local concentration of the histidine side chains relative to the heme. In turn, the local concentration of a histidine ligand provides information about the statistical nature of the polypeptide chain segment separating the heme and the histidine ligand. Results reported here use imidazole titrations of unfolded cytochrome c to estimate, relative to the heme, the effective concentrations of histidine side chains at three positions in the polypeptide chain. High denaturant concentrations are employed, and under these conditions, the results are in general agreement with the random-coil model for the unfolded protein.

Materials and Methods

Growth of Yeast and Protein Purification. Growth of yeast and protein purification and characterization have been described previously (Nall & Landers, 1981; Wood et al., 1988). Yeast strain B4926 (α CYC7-H1 cyc1-1 trp1-1) was used to obtain iso-2-cytochrome c, and strain D273-11A (α ade1 his1) was used for iso-1.[1] Both strains were gifts from Fred Sherman (University of Rochester School of Medicine and Dentistry). Yeast were grown on YPD medium (1% yeast extract, 0.25% peptone, and 1% dextrose). Standard YPD medium contains 2% peptone and 2% dextrose (Sherman et al., 1974). The peptone was reduced to lower costs. Lower amounts of dextrose were used to improve cytochrome c induction which occurs only after the dextrose is depleted from the medium. Iso-1-MS was prepared by reacting iso-1 with methyl methanethiosulfonate (MS) to block Cys-102 (Ramdas et al., 1986) and eliminate disulfide dimer formation between iso-1 monomers. Tuna cytochrome c was obtained from Sigma.

NMR Measurements. Samples were prepared from lyophilized protein at a concentration of 1–3 mM in 99.7% D_2O (Cambridge Isotopes) and 0.1 M sodium phosphate, pD 7.2. Fully deuterated imidazole (98% D, imidazole-D_4, KOR Isotopes) was used to minimize interference from proton resonances from the added imidazole. Nevertheless, at high imidazole concentrations, resonances from residual protonated imidazole are observed. Sample pD (meter readings, not corrected for isotope effects) was adjusted with deuterium chloride. The temperature was regulated at 20 and 30 °C.

Spectra were obtained on a JEOL GX-270WB spectrometer with a variable-temperature 5-mm $^1H/^{13}C$ probe. Proton ($\pi/2$) pulse widths were 15–18 μs. A selective 100-ms presaturating pulse was applied at the HOD frequency to reduce the intensity of the residual HOD signal. The presaturating pulse was also effective in reducing the residual amide proton resonance from Gdn·HCl by cross-saturation from HOD. Proton NMR spectra were obtained by Fourier transformation of signal-averaged free induction decays. Typically, 32K data points were collected with quadrature detection and a 30-kHz frequency bandwidth. Chemical shifts are relative to an internal [$^2H_4$]TSP standard which was added to the samples at a molar ratio of about 0.05 of that of the protein.

Results

Imidazole Titrations. Figure 1 shows a titration of guanidine hydrochloride unfolded yeast iso-2-cytochrome c over a 0–100 mM concentration range of deuterated imidazole. As

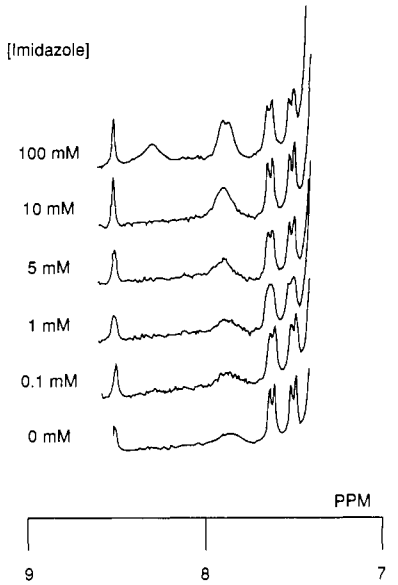

FIGURE 1: Titration of unfolded iso-2-cytochrome c with deuterated imidazole. The histidine ring C_2H region of the proton NMR spectrum for iso-2-cytochrome c is shown as a function of deuterated imidazole concentration in the presence of 3.5 M Gdn·DCl and 0.1 M sodium phosphate, pD 7.2, at 30 °C. Resonances in the 7.8–7.9 ppm region which increase in intensity with increasing imidazole concentration are ring C_2H protons from histidine side chains displaced from the heme by imidazole. The broad resonance near 8.3 ppm seen only at 100 mM deuterated imidazole is from residual protonated imidazole.

Table I: Number and Location of Histidine Residues in Cytochromes c[a]

protein	amino acid/position			
	-17-18-19-	-25-26-27-	-32-33-34-	-38-39-40-
iso-1-MS (4 His)	-C-H-T	-P-H-K-	-L-H-G-	-R-H-S-
iso-2 (3 His)	-C-H-T-	-P-N-K-	-L-H-G-	-R-H-S-
tuna (2 His)	-C-H-T-	-K-H-K-	-L-W-G-	-R-K-T-

[a] Locations of histidine residues and their nearest neighbors are shown for three types of mitochondrial cytochromes c (Dickerson, 1972; Hampsey et al., 1986; Montgomery et al., 1980).

the imidazole concentration increases, a broad resonance near 7.8–7.9 ppm increases in intensity and splits into two resonances. At the highest imidazole concentration (100 mM), a resonance near 8.3 ppm appears which control spectra show is from residual protonated imidazole. Two split single proton resonances near 7.4 and 7.6 ppm are useful as area standards and have the chemical shifts expected for the indole ring C_4H and C_7H protons of Trp-59. A similar titration of yeast iso-1-MS cytochrome c shows some qualitative differences. Two, near full intensity resonances are observed even in the absence of imidazole. At high imidazole concentration, a third resonance appears which is probably His-26 (see Discussion).

Correlations of Spectra with the Number of Histidines. In Figure 2, spectra at high imidazole concentration (150 mM) are shown for unfolded iso-1-MS, iso-2, and tuna cytochromes c. These proteins contain, respectively, four, three, and two histidine residues (see Table I). Titrations show that at 150 mM imidazole the system is approaching saturation in that the number and intensity of the histidine C_2H resonances (7.8–7.9 ppm region) change little as the imidazole concentration is raised above 100 mM imidazole. There are three histidine C_2H resonances for iso-1-MS, two for iso-2, and one for tuna cytochrome c. Interestingly, the number of C_2H resonances appearing in the diamagnetic region of the spectrum is one less than the total number of histidines in the particular variety of cytochrome c. This suggests that all but one of the histidine residues are displaced from the heme by

[1] Abbreviations: Gdn·HCl, guanidine hydrochloride; Gdn·DCl, deuterated guanidine hydrochloride; MS, methyl methanethiosulfonate; iso-2, iso-2-cytochrome c from the yeast *Saccharomyces cerevisiae*; iso-1, iso-1-cytochrome c from the yeast *Saccharomyces cerevisiae*; iso-1-MS, iso-1 treated with methyl methanethiosulfonate; NMR, nuclear magnetic resonance; [$^2H_4$]TSP, sodium 3-(trimethylsilyl)tetradeuteriopropionate; D_2O, deuterium oxide; pD, uncorrected pH meter reading for a deuterium oxide solution; Hz, hertz (s^{-1}).

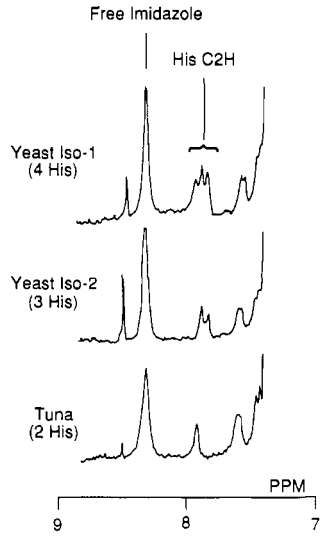

FIGURE 2: Nuclear magnetic resonance (NMR) spectra of unfolded cytochromes *c* in the presence of saturating imidazole. Spectra of iso-1-MS, iso-2, and tuna cytochromes *c* are shown in the presence of 3.5 M deuterated guanidine hydrochloride, 150 mM deuterated imidazole, and 0.1 M sodium phosphate, pD 7.2 at 30 °C. These three members of the mitochondrial cytochrome *c* family have four, three, and two histidine residues, respectively. The high concentration of guanidine hydrochloride is sufficient to fully unfold the proteins to an unstructured state containing histidine side chains as heme ligands at the fifth and sixth coordination positions. In the absence of imidazole, the resonances from histidine heme ligands are shifted and broadened by the heme paramagnetism and are missing in the histidine ring C_2H proton region. At a concentraion of 150 mM, the deuterated imidazole binds to the heme iron atom, displacing histidine ligands so that the ring C_2H resonances appear in the diamagnetic spectral region. The number of resonances is one less than the total number of His side chains in a given cytochrome *c* variant, suggesting that one histidine side chain remains as a heme ligand (see text). Resonance positions are indicated for an imidazole proton and for the histidine C_2H ring protons. The imidazole is fully deuterated at the 98% level and is not seen in the proton NMR spectra at low imidazole concentrations. However, contaminating protonated imidazole shows up as a strong resonance in the proton NMR spectrum at high imidazole concentrations.

addition of imidazole. Although all of the proteins are at Gdn·DCl concentrations above the cooperative unfolding transition zone, the displaced C_2H resonances show slight differences in chemical shift. The chemical shift differences could indicate residual structure but more likely reflect histidine p*K* differences resulting from the different neighboring amino acids for histidines at different sequence positions (Table I).[2]

Discussion

Retention of the His-18 Ligand at High Imidazole Concentration? Since the number of ring C_2H resonances observed at high imidazole concentration is one less than the number of histidine side chains (Figure 2), the simplest conclusion is that one histidine is retained as a heme ligand and the corresponding C_2H resonance remains in the paramagnetic region of the NMR spectrum. The existing data do not provide direct proof of the identity of this ligand, but there are several reasons why His-18 is the most likely candidate. First, at high imidazole concentration, all three varieties of unfolded cytochromes *c* are short one C_2H ring resonance, and His-18 is the only histidine all three cytochromes *c* have in common (Table I) (Dickerson, 1972; Hampsey et al., 1986; Montgomery et al., 1980). Second, His-18 is adjacent to one of the two Cys side chain thioether links that covalently attach the heme to the polypeptide chain, so His-18 is closer in the linear sequence to the heme than any of the other histidines. Finally, His-18 is a heme ligand in native cytochrome *c* (Takano & Dickerson, 1981a,b), so local peptide chain conformations are known to accommodate, if not facilitate, ligation by His-18. Thus, at least one local chain conformation allows ligation, so effective concentrations of His-18 might well exceed attainable imidazole concentrations.

Table II: Tentative Resonance Assignments and pK_d Estimates for Histidine Side Chains

amino acid residue[a]	σ_{obs} (ppm)[a]	f_{His^+}[b]	pK_d[c]
His-33	7.82	0.14	6.40
His-39	7.87	0.19	6.56
His-26	7.93	0.25	6.71

[a] Resonance assignments are for unfolded cytochromes *c*, 30 °C, pD 7.2, in the presence of 3.5 M Gdn·HCl and 150 mM imidazole. Chemical shifts are expressed relative to an internal TSP reference. Assignments are based on comparisons of NMR spectra for cytochrome *c* sequence variants and on expected pK_d differences from neighboring charged side chains (see text and Table I). Our analysis of chemical shift differences assumes that σ_{His^+} and σ_{His} are independent of sequence. Differences of σ_{obs} are assumed to arise from changes in p*K* induced by local structure or sequence. [b] f_{His^+} is the fraction of the histidine side chain in the protonated form. $f_{His^+} = (\sigma_{His^+} - \sigma_{obs})/(\sigma_{His^+} - \sigma_{His})$, where σ_{His} = 7.68 ppm and σ_{His^+} = 8.70 ppm are the chemical shifts of the fully deprotonated and fully protonated forms of the histidine side chains, respectively (Wuthrich, 1976). [c] pK_d values are apparent values in D_2O in the presence of 3.5 M Gdn·HCl, 30 °C. They are calculated from $pK_d = 7.2 - \log [(1 - f_{His^+})/f_{His^+}]$.

Tentative Sequence-Specific Assignments for Displaced Histidine Ligands. At first, it seems surprising that ring C_2H resonances show chemical shift differences in Gdn·DCl-unfolded cytochrome *c*. In the absence of organized structure, side-chain environments and the resulting chemical shifts should be very similar. However, pD = 7.2 is not far removed from the pK_d for deprotonation of a histidine ring, so local sequence differences affecting the pK_d will give protonation-induced chemical shift differences. In Table II, the chemical shifts of the three displaced histidine side chains are listed along with estimates for pK_d and the fraction protonated (pD 7.2, 30 °C). The pK_d values are estimated by assuming the chemical shifts from model compound studies for the fully protonated and fully deprotonated forms of the side chain (Wuthrich, 1976). Iso-2 is the only variant with Asp in place of His at position 26, so His-26 can be assigned by comparing spectra for iso-1-MS, tuna cytochrome *c*, and iso-2. His-33 and His-39 are assigned on the basis of expected pK_d differences. His-39 is preceded by a positively charged arginine in the linear sequence, so the pK_d for His-39 should be lower than that for His-33, which has uncharged nearest neighbors (Table I). On the basis of model spectra of protonated and deprotonated forms of histidine (Wuthrich, 1976), the histidine with the lower pK_d will also have a lower chemical shift. These assignments must be considered very tentative, but provide a reasonable framework for interpretation of available data.

Sharing of Heme–His Ligands in Unfolded Iso-2. Optical spectroscopy shows that the heme in unfolded cytochrome *c* is in a low-spin state (Babul & Stellwagen, 1971). Since heme ligation by water gives a high-spin heme, the heme–ligand complex must involve low-spin heme ligands from protein side chains. It has long been assumed that histidine side chains

[2] The vertebrate cytochrome *c* numbering system is used to denote amino acid positions in order to facilitate comparison between members of the cytochrome *c* family. Iso-2 has nine additional amino-terminal residues and one residue less on the carboxy terminus compared to vertebrate cytochromes *c*. Thus, the vertebrate numbering of iso-2 starts at position −9 and extends to position 103 [see Dickerson (1972) and Hampsey et al. (1986)]. For example, Tyr-67 in the vertebrate numbering system corresponds to Tyr-76 in the iso-2 numbering system.

were heme ligands in unfolded cytochrome *c*, a suggestion strongly supported by the present data. Less clear is whether unfolded cytochromes *c* have a unique set of histidine heme ligands. Sequence comparisons among the three cytochrome *c* variants show that different unfolded proteins must differ in the identity of at least one histidine heme ligand. For example, assuming His-18 is always one ligand, the remaining ligand must be His-26 in tuna cytochrome *c* but cannot be His-26 in iso-2 since iso-2 has asparagine at position 26 (Table I). An equally important question is whether unfolded cytochromes *c* with three or more histidines have one or multiple heme ligand states in the unfolded protein. The imidazole titration of iso-2 (Figure 1) shows clearly that the three histidines share the two heme ligation sites. There are no full intensity diamagnetic C_2H resonances at zero or low imidazole concentrations, so each of the three histidines is a heme ligand at least part of the time. If His-18 is assumed to always be a ligand, then His-33 and His-39 share the one remaining heme ligation site.

Association Constants for Binding of Imidazole. The data in Figure 2 allow calculation of an approximate association constant for the reaction:

$$U + I = U\text{–}I \qquad (1)$$

where U is the unfolded cytochrome *c* concentration, I is the imidazole concentration, and U–I is the concentration of the complex between unfolded cytochrome *c* and imidazole. Note that a binding stoichiometry of 1 to 1 is assumed, as indicated by the number of full intensity C_2H resonances observed at saturating imidazole. The equilibrium binding constant can be expressed in terms of the total imidazole, I_T, total unfolded protein, U_T, and fraction of protein complexed with imidazole, f_B:

$$K_B = (U\text{–}I)/UI = f_B/[(1 - f_B)(I_T - f_B U_T)] \qquad (2)$$

K_B can be estimated at half-saturation, where $f_B = {}^1/_2$. Taking $U_T = 2 \times 10^{-3}$ M and $I_T \sim 7.9 \times 10^{-3}$ M, a value of $K_B \sim 1.45 \times 10^2$ L/M is obtained for iso-2 at 30 °C, pD 7.2. A similar estimate based on titration of iso-1-MS with imidazole gives $K_B \sim 35.4$ L/M for iso-1-MS at 20 °C, pD 7.2. The difference in K_B values for the two proteins is in the expected direction. Binding should be weaker to iso-1-MS since it contains an additional competing side chain (His-26) that is lacking in iso-2 (Table I).

Estimation of Effective Concentrations. Table III lists the effective concentrations of histidine side chains relative to the heme ligation site. In all cases, His-18 is assumed to be a nondisplaceable heme ligand with an effective concentration above that measured by the imidazole titrations (for His-18, $c^{eff} > 191 \times 10^{-3}$ M). The total effective concentration c^{eff}_{tot} is taken as the imidazole concentration that gives half-saturation of the heme ligation site as judged by histidine ring C_2H resonance intensities. Since His-18 remains as a heme ligand, c^{eff}_{tot} contains only contributions from the displaceable histidines: all histidines other than His-18. Effective concentrations for individual histidine side chains are estimated by assuming that the polypeptide separating each histidine and the heme behaves as an unperturbed statistical polymer chain. More specifically, we assume that the effective concentration of a given histidine side chain relative to the heme is proportional to the number of amino acids in the loop formed by heme ligation raised to the $-{}^3/_2$ power (see Table III) (Flory, 1953). While admittedly a rough approximation, the unperturbed chain assumption provides a means of apportioning the total effective concentration among the contributing histidine side chains. A partial test of the assumption is given by comparing effective concentrations obtained for iso-1-MS vs iso-2 for His-33 and His-39 [$c^{eff}(18)$ and $c^{eff}(24)$, respectively]. $c^{eff}(18)$ and $c^{eff}(24)$ will differ slightly from each other because of different ligation loop lengths, but the values for each should be the same in iso-1-MS and iso-2. The values are of the same order of magnitude in both proteins (Table III) but are not identical. This suggests that the estimates for the effective concentrations of specific side chains have errors of about a factor of 2, probably arising from both experimental errors and an overly simplified model.

Table III: Estimation of Effective Concentrations of His Side Chains Relative to Heme

	residue			
protein	all[a] c^{eff}_{tot} (M/L)	His-26 $c^{eff}(11)$ (M/L)[b]	His-33 $c^{eff}(18)$ (M/L)[b]	His-39 $c^{eff}(24)$ (M/L)[b]
iso-2[c]	7.9×10^{-3}	$[9 \times 10^{-3}]$[a]	4.7×10^{-3}	3.2×10^{-3}
iso-1-MS[c]	29×10^{-3}	16×10^{-3}	7.8×10^{-3}	5.1×10^{-3}

[a] His-18 is assumed to always be a heme ligand, so estimates of the total effective concentration of histidine side chains (c^{eff}_{tot}) relative to the single remaining heme ligation site are the sum of the effective concentrations of all histidines in the protein other than His-18. For iso-1-MS, this includes histidines at positions 26, 33, and 39. For iso-2, with asparagine at position 26 (Table I), His-33 and His-39 contribute to c^{eff}_{tot}. Experimentally, c^{eff}_{tot} is taken to be equal to the imidazole concentration giving half-saturation. [b] Effective concentrations for individual side chains relative to the heme are estimated by solving the following equations: (1) $c^{eff}_{tot} = \sum_i c^{eff}_i$ where the sum is over all histidines; (2) $c^{eff}_i/c^{eff}_k = (n_i/n_k)^{-3/2}$ where $n_{i,k}$ is the number of amino acids in the loop formed when histidine i (or k) binds to the heme. Since the heme is attached to the polypeptide chain at both position 14 and position 17, there is some ambiguity regarding the exact location of the heme. We have taken position 16 as the location of the heme, giving loop lengths of $n = 11$, 18, and 24 for His-26, His-33, and His-39, respectively. [c] Titration of iso-1-MS was at 20 °C, and titration of iso-2 was at 30 °C. Titrations of both iso-1-MS and iso-2 were in the presence of 3.5 M Gdn·DCl and 0.1 M sodium phosphate, pD 7.2.

Conclusions

The results provide strong additional support for the notion that two histidine side chains are heme ligands in unfolded cytochrome *c* at neutral pH. One histidine, probably His-18, has an intramolecular effective concentration relative to the heme in excess of 191×10^{-3} M. Additional histidines share the one remaining heme ligation site as determined by their respective effective concentrations which are in the range of $(3\text{–}16) \times 10^{-3}$ M. Assuming the validity of tentative residue-specific resonance assignments, the intramolecular effective concentrations for histidine side chains relative to the heme have the order His-18 $\gg$ His-26 > His-33 $\sim$ His-39. With only minor discrepancies, the results are consistent with those expected for a random-coil polymer.

Acknowledgments

Professor Finn Wold is thanked for support and encouragement with regard to NMR spectroscopy. The NMR spectroscopy was carried out in the NMR spectroscopy facility of the Department of Biochemistry and Molecular Biology at the University of Texas Health Science Center, Houston. This facility was established with partial support from the Robert Welch Foundation.

Registry No. His, 71-00-1; heme, 14875-96-8; cytochrome *c*, 9007-43-6; imidazole, 288-32-4.

References

Babul, J., & Stellwagen, E. (1971) *Biopolymers 10*, 2359–2361.

Brandts, J. F. (1969) in *Structure and Stability of Biological Macromolecules* (Timasheff, A., & Fassman, G. D., Eds.)

pp 213-290, Marcel Dekker, Inc., New York.
Brems, D. N., & Stellwagen, E. (1983) *J. Biol. Chem. 258*, 3655-3660.
Dickerson, R. E. (1972) *Sci. Am. 226*, 58-72.
Flory, P. J. (1953) *Principles of Polymer Chemistry*, 1st ed., Cornell University Press, Ithaca, NY.
Hampsey, D. M., Das, G., & Sherman, F. (1986) *J. Biol. Chem. 261*, 3259-3271.
Montgomery, D. L., Leung, D. W., Smith, M., Shalit, P., Faye, G., & Hall, B. D. (1980) *Proc. Natl. Acad. Sci. U.S.A. 77*, 541-545.
Myer, Y. P. (1984) *J. Biol. Chem. 259*, 6127-6133.
Nall, B. T., & Landers, T. A. (1981) *Biochemistry 20*, 5403-5411.
Ramdas, L., Sherman, F., & Nall, B. T. (1986) *Biochemistry 25*, 6952-6958.
Sherman, F., Fink, G. R., & Lawrence, C. W. (1974) *Methods in Yeast Genetics* (revised 1979 ed.), Cold Spring Harbor Laboratory, Cold Spring Harbor, NY.
Shortle, D., & Meeker, A. K. (1986) *Proteins: Struct., Funct., Genet. 1*, 81-89.
Shortle, D., & Meeker, A. K. (1989) *Biochemistry 28*, 936-944.
Takano, T., & Dickerson, R. E. (1981a) *J. Mol. Biol. 153*, 95-115.
Takano, T., & Dickerson, R. E. (1981b) *J. Mol. Biol. 153*, 79-94.
Wood, L. C., Muthukrishnan, K., White, T. B., Ramdas, L., & Nall, B. T. (1988) *Biochemistry 27*, 8554-8561.
Wuthrich, K. (1976) *NMR in Biological Research: Peptides and Proteins*, 1st ed., North-Holland Publishing Co., Amsterdam and Oxford.

Assembly of the F_o Proton Channel of the *Escherichia coli* F_1F_o ATPase: Low Proton Conductance of Reconstituted F_o Sectors Synthesized and Assembled in the Absence of F_1†

Sushma Pati‡ and William S. A. Brusilow*

Department of Biochemistry, Wayne State University School of Medicine, Scott Hall, 540 East Canfield Avenue, Detroit, Michigan 48201

Gabriele Deckers-Hebestreit and Karlheinz Altendorf

Department of Microbiology, Universität Osnabrück, Barbarastrasse 11, D-4500 Osnabrück, Germany

Received November 7, 1990; Revised Manuscript Received February 19, 1991

ABSTRACT: We have previously proposed that during assembly of the *Escherichia coli* F_1F_o ATPase, the proton permeability of the F_o sector of the *E. coli* F_1F_o ATPase is increased significantly by interactions with F_1 subunits [Pati, S., & Brusilow, W. S. A. (1989) *J. Biol. Chem 264*, 2640-2644]. To test this model for F_o assembly, we purified F_o sectors synthesized in the presence and absence of F_1 subunits and measured the abilities of these different preparations to bind purified F_1 ATPase and to conduct protons when reconstituted into liposomes. The results of these studies demonstrated significant differences in proton-conducting abilities of the different F_o preparations. F_o sectors synthesized in the presence of F_1 subunits were more permeable to protons than those synthesized in the absence of F_1 subunits.

The proton-translocating F_1F_o ATPase of *Escherichia coli* consists of an intrinsic membrane-bound sector, F_o, which forms a proton channel across the cytoplasmic membrane and an extrinsic sector, F_1, which catalyzes ATP synthesis or hydrolysis [for reviews, see Schneider and Altendorf (1987) and Futai et al. (1989)]. The F_o consists of three different subunits (a, b, and c), and the F_1 consists of five different subunits (α, β, γ, δ, and ϵ). The subunits are present in different numbers in the complex, and the stoichiometry has been shown to be $a_1b_2c_{10}\alpha_3\beta_3\gamma_1\delta_1\epsilon_1$ (Foster & Fillingame, 1982). The synthesis, membrane insertion, and assembly of these different subunits into functional F_1, F_o, and F_1F_o complexes must be accomplished without the formation of harmful intermediates which might disrupt the transmembrane proton gradient, deplete cellular ATP levels, or both. A model proposed by Cox et al. (1981; Cox & Gibson, 1987) described an assembly pathway in which certain F_o subunits would not be assembled into the membrane in the absence of certain F_1 subunits, thereby eliminating the possibility of either the F_o or the F_1 assembling in the absence of the other. Subsequent studies from other laboratories, however, demonstrated that reconstitutable F_o could be synthesized and assembled in the absence of F_1 (Aris et al., 1985; Fillingame et al., 1986). Genetic studies by Brusilow (1987) concluded that the presence of F_1 subunits could significantly affect the proton permeability of F_o sectors synthesized from genes on multicopy plasmids, and Pati and

†This research was presented as part of the Ph.D. thesis of S.P. (University of Maryland, 1990). This research was supported by National Science Foundation Grant DMB-8805416 and by American Heart Association Grant-in-Aid 87-1297, with funds contributed by the AHA Maryland Affiliate, Inc. W.S.A.B. is the recipient of U.S. Public Health Service Research Career Development Award NIH KO4-AI00882. Further support came from the Deutsche Forschungsgemeinschaft (SFB 171/B4), the Niedersächsische Ministerium für Wissenschaft und Kultur, and the Fonds der Chemischen Industrie.

*To whom correspondence should be addressed.

‡Present address: Genetics and Biochemistry Branch, National Institutes of Diabetes and Digestive and Kidney Diseases, NIH, Bethesda, MD 20892.

0006-2960/91/0430-4710$02.50/0